Cooperative Wireless Powered Communication Networks With Interference Harvesting

Wonjae Shin, *Member, IEEE*, Mojtaba Vaezi, *Member, IEEE*, Jungwoo Lee, *Senior Member, IEEE*, and H. Vincent Poor, *Fellow, IEEE*

***Abstract*—A cooperative wireless-powered communication network protocol is proposed, in which user far away from a hybrid access point (H-AP) is capable of harvesting wireless powers by overhearing the uplink signals of users that are relatively nearer to the H-AP, in addition to downlink signal broadcast by the H-AP. In this setting, time allocations for the downlink transmission of the H-AP and the uplink transmission for the users are jointly optimized for two different purposes. First, the *weighted sum-rate maximization* problem is solved for a given total transmission time. Then, the *total transmission time* is minimized under a minimum rate constraint, and an efficient algorithm is also presented to solve the optimal solution by a line search strategy. Numerical results demonstrate that the proposed schemes significantly increase the far user's rate, which in turn improves user fairness and transmission delay.**

***Index Terms*—Wireless powered communication networks, user cooperation, user fairness, transmission delay.**

I. Introduction

To enable reliable and self-sustainable wireless networks for fifth generation (5G) cellular systems, such as the Internet-of-things (IoT), energy harvesting technologies [1]–[3] have recently drawn significant attention in both academia and industry. In particular, wireless powered communication networks (WPCNs) [4]–[6] represent a promising new paradigm in the design of wireless networks, in which wireless devices are powered over the air by dedicated wireless power transmitters for information transmissions without the need for manual battery replacement/recharging. A joint optimized design of energy transfer and information transmission [6] has been recently studied to improve the user throughput in WPCNs, where a hybrid access point (H-AP) acts not only as a power transmitter but also as an information receiver. Due to a significant signal power attenuation over distance, the harvested energy level at a user far from the H-AP is much less than that of near users; however, relatively more energy is required to send a far user's information to the H-AP. This phenomenon, which is called *doubly near-far problem* in WPCNs [6], causes severe throughput disparity among the users in different locations and is related to user fairness.

Manuscript received May 20, 2017; revised October 1, 2017; accepted November 19, 2017. Date of publication December 19, 2017; date of current version April 16, 2018. The work of W. Shin and J. Lee was supported by the Basic Science Research Program (NRF-2017R1A2B2007102) through the National Research Foundation of Korea by the Minister of Science, ICT, and Future Planning (MSIP). The work of M. Vaezi and H. V. Poor was supported by the U.S. Army Research Office under Grant W911NF-16-1-0448. The review of this paper was coordinated by Prof. W. Choi. *(Corresponding author: Jungwoo Lee.)*

W. Shin is with the Department of Electrical Engineering, Princeton University, Princeton, NJ 08544, USA and also with the Department of Electronics Engineering, Pusan National University, Pusan 46241, Korea (e-mail: wjshin@pusan.ac.kr).

M. Vaezi and H. V. Poor are with the Department of Electrical Engineering, Princeton University, Princeton, NJ 08544, USA (e-mail: mvaezi@princeton.edu; poor@princeton.edu).

J. Lee is with the Department of Electrical and Computer Engineering, Seoul National University, Seoul 08826, South Korea (e-mail: junglee@snu.ac.kr).

Color versions of one or more of the figures in this paper are available online at http://ieeexplore.ieee.org.

Digital Object Identifier 10.1109/TVT.2017.2785318

To overcome this critical issue in WPCNs, various potential solutions have been recently introduced under different setups. One popular approach is the use of energy beamforming with a multiple-antenna H-AP so that the amount of energy transferred to users can be controlled by the H-AP [7]. In general, for energy beamforming, the H-AP requires to receive accurate channel state information to all users through uplink feedback. Considering the channel feedback overheard, this might even degrade the uplink rate performance in IoT scenarios which support very large numbers of small devices. Non-orthogonal multiple access has also been applied in the context of WPCN to enhance spectral efficiency and user fairness [8], [9].

On the other hand, cooperative relay protocols for WPCNs have been developed in [10] from the intuition that a near user can help a far user by forwarding the far user's message in addition to its own message to the H-AP. The cooperation benefit comes from the fact that the near user has much higher efficiency in both energy transfer and information transmission due to its shorter distance compared to far users. However, the implementation of cooperative relaying can be very costly due to its practical requirements for the operation, such as high computational complexity for decoding, transmission delay, and signaling overhead.[1] In [11], a dedicated relay is considered to help a far user rather than a near user. In contrast, the concept of energy cooperation protocol has been proposed [5], [12] so that the near user directly shares its excessive energy with far users via (orthogonal) out-of-band channels, instead of information forwarding. In fact, the potential gain from energy cooperation can be dramatically compromised by a large amount of overhead for the extra spectrum resources.

In this paper, we continue to explore the benefit of cooperative protocols in WPCNs yet from a different perspective. We propose a novel cooperative WPCN framework, in which the far users can consistently scavenge energy by overhearing signals sent by nearer users to the H-AP before its information transmission. This cooperative protocol can significantly improve user fairness while it does not sacrifice the near user's energy and rate in contrast to most prior work. Under this new setting, we are interested in jointly optimizing time allocations for the downlink transmission of the H-AP and the uplink transmission for the users. It is worth emphasizing that the system model in this paper is quite different from that of the conventional WPCN with an ambient interfering source (see for example [9] and the references therein).

The contributions of this paper are three-fold: First, we propose a novel cooperative WPCN concept by embracing interference from nearer users to harvest energy at the users. Second, for the cooperative WPCN, we formulate a weighted sum-rate maximization problem, and present an optimal time allocation in closed form. Lastly, we find an optimal solution of a total time minimization problem in closed form, which is targeted for low latency IoT applications.

II. System Model

As shown in Fig. 1, we consider a cooperative WPCN, consisting of one H-AP and K users operating in the same frequency band.[2] The H-AP is connected to a constant power supply, while each

[1] All active users as well as the H-AP in a WPCN must be aware of the other users' codebooks and control information on scheduling/resource allocation at all time, which incurs a significant signaling overhead in practice.

[2] The power transfer efficiency can be improved particularly for a narrowband link, although not for a broadband data link [13], if the power and data transfer functions of a wireless link are separated; yet, this brings some new practical challenges for low-cost IoT devices.

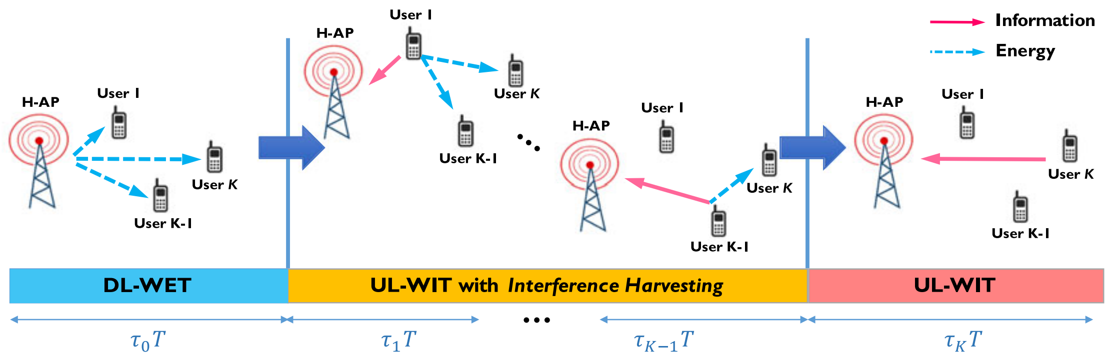

Fig. 1. An illustration of cooperative WPCN with interference harvesting, where DL-WET and UL-WIT refer to wireless energy transfer in the downlink and wireless information transmission in the uplink, respectively.

user has a supercapacitor as an energy storage to accumulate the energy harvested from the environment, but no external power supply [14].[3]

It is assumed that the H-AP and users are each equipped with a single antenna. Furthermore, we assume block based transmissions over quasi-static flat-fading channels in which channel coefficients remain constant during each block transmission time, denoted by T. The channel power gain between the H-AP and user i is denoted by h_i for both the downlink and uplink due to the channel reciprocity. Without loss of generality, it is assumed that the users are sorted in the descending order of channel gains, i.e., $|h_i| \geq |h_j|$ for $i < j$. Also, $g_{i,\ell}$ represents the channel power gain between user i and user ℓ.

In each block, the first $\tau_0 T$ amount of time is assigned to the downlink transmission for the H-AP to broadcast wireless energy to all users where $\tau_0 \in [0, 1]$. The remaining time in the same block is assigned to the uplink channel for information transmission, in which each user sends its independent information to the corresponding H-AP by time division multiple access (TDMA). The amount of time allocated to the transmission of user i is denoted as $\tau_i T$, $i = 1, \ldots, K$. Note that we have a total and individual time constraints as follows:[4]

$$\sum_{i=0}^{K} \tau_i \leq 1, \quad \text{and} \quad \tau_i \geq 0. \tag{1}$$

During the $(i+1)$th time slot, users with relatively poor channel conditions compared to the ith user harvest energy by overhearing the signal sent by the ith user, with the aim of alleviating the doubly near-far problem in WPCNs [6]. By doing so, user i can transmit its own information to the H-AP using the accumulated harvested energy during the previous $\sum_{i=0}^{i-1} \tau_i T$ amount of time.[5] Due to the significant self-discharge of the supercapacitor, it is reasonable to assume that the energy harvested after data transmission in each block cannot be utilized in the next block. Then the average transmit power at user i, denoted as $P_i(\boldsymbol{\tau})$, is given as follows:

$$P_i(\boldsymbol{\tau}) = \eta \frac{P_0 h_i \tau_0 + \sum_{\ell=1}^{i-1} P_\ell(\boldsymbol{\tau}) g_{i,\ell} \tau_\ell}{\tau_i} \tag{2}$$

$$= \frac{\eta h_i \mathbf{e}_0 \boldsymbol{\tau}}{\mathbf{e}_i \boldsymbol{\tau}} P_0 + \sum_{\ell=1}^{i-1} \frac{\eta g_{i,\ell} \mathbf{e}_\ell \boldsymbol{\tau}}{\mathbf{e}_i \boldsymbol{\tau}} P_\ell(\boldsymbol{\tau}), \tag{3}$$

where $\boldsymbol{\tau} = [\tau_0, \ \tau_1, \ldots, \tau_K]^T$, and $\mathbf{e}_i$ denotes a row vector of length $K + 1$ with 1 in the $(i + 1)$th position and 0 in every other positions.

[3] Supercapacitors have the advantages of small form factor and rapid charging with a great number of charging cycles; however, they suffer from considerably high self-discharge and leakage.

[4] Note that the total time constraint is no longer valid in Section IV.

[5] According to [6]–[11], it is assumed that the energy harvested from the noise at the users is negligible.

Also, η denotes the energy conversion efficiency at the receiver, $\eta \in (0, 1)$.[6] In this regard, latter users have more opportunity to harvest energy with the help of the proposed cooperation protocol, and can achieve a better balanced rate as compared with basic WPCN. For convenience, we use a normalized unit block time, i.e., $T = 1$.

Assuming an additive white Gaussian noise at the H-AP receiver, the achievable rate of user i through uplink information transmission within a block is given by

$$R_i(\boldsymbol{\tau}) = \mathbf{e}_i^T \boldsymbol{\tau} \log_2 \left(1 + \frac{P_i(\boldsymbol{\tau}) h_i}{\sigma^2}\right), \quad i = 1, \ldots, K, \tag{4}$$

where σ^2 denotes the noise power at the H-AP.

III. A Weighted Sum-Rate Maximization

In this section, we maximize the weighted sum-rate of the cooperative WPCN, which is formulated as

$$(\mathbf{P1}): \quad \max_{\boldsymbol{\tau}} \sum_{i=1}^{K} \omega_i R_i(\boldsymbol{\tau}), \tag{5}$$

$$\text{s.t.} \quad \mathbf{1}^T \boldsymbol{\tau} \leq 1, \tag{6}$$

$$\mathbf{e}_i^T \boldsymbol{\tau} > 0, \quad i = 0, 1, \ldots, K, \tag{7}$$

$$\omega_i \geq 0, \quad i = 1, 2, \ldots, K, \tag{8}$$

where $\mathbf{1}$ denotes an all-one vector with an appropriate dimension.

It is a non-trivial task to show the convexity of the objective function of $(\mathbf{P1})$ with respect to $\boldsymbol{\tau}$ in the above form since $P_i(\boldsymbol{\tau})$ is a recursive function. To simplify this, we define the new variable $\gamma_i \triangleq P_i(\boldsymbol{\tau}) \frac{\mathbf{e}_i^T \boldsymbol{\tau}}{\mathbf{e}_0^T \boldsymbol{\tau}} \frac{h_i}{\sigma^2}$.

Lemma 1: Given $\gamma_0 = 0$, γ_i can be expressed in the recursive form $\gamma_i = \frac{\eta P_0 h_i^2}{\sigma^2} + \eta \sum_{\ell=1}^{i-1} \left(\frac{g_{i,\ell} h_i}{h_\ell}\right) \gamma_\ell$, which is constant with respect to $\boldsymbol{\tau}$.

Proof: According to the definition of γ_i, the following relation holds:

$$\gamma_i = \frac{\mathbf{e}_i^T \boldsymbol{\tau}}{\mathbf{e}_0^T \boldsymbol{\tau}} \frac{P_i(\boldsymbol{\tau}) h_i}{\sigma^2}$$

$$\overset{(a)}{=} \eta \frac{\mathbf{e}_i^T \boldsymbol{\tau}}{\mathbf{e}_0^T \boldsymbol{\tau}} \frac{\frac{h_i^2 \mathbf{e}_0^T \boldsymbol{\tau}}{\mathbf{e}_i^T \boldsymbol{\tau}} P_0 + \sum_{\ell=1}^{i-1} \frac{g_{i,\ell} h_i \mathbf{e}_\ell^T \boldsymbol{\tau}}{\mathbf{e}_i^T \boldsymbol{\tau}} P_\ell(\boldsymbol{\tau})}{\sigma^2}$$

$$\overset{(b)}{=} \frac{\eta P_0 h_i^2}{\sigma^2} + \eta \sum_{\ell=1}^{i-1} \left(\frac{g_{i,\ell} h_i}{h_\ell}\right) \gamma_\ell, \tag{9}$$

[6] For convenience of exposition, it is assumed that the energy harvesting efficiency is identical for all user terminals.

where (a) comes from the expression for $P_i(\boldsymbol{\tau})$ in (3), and (b) follows from the definition of γ_ℓ. It can be seen that, in the end, γ_i is not a function of $\boldsymbol{\tau}$.

From Lemma 1, the rate of $R_i(\boldsymbol{\tau})$ can be re-expressed as

$$R_i(\boldsymbol{\tau}) = \mathbf{e}_i^T\boldsymbol{\tau}\log_2\left(1+\gamma_i\frac{\mathbf{e}_0^T\boldsymbol{\tau}}{\mathbf{e}_i^T\boldsymbol{\tau}}\right), \tag{10}$$

where $\gamma_i = \frac{\eta P_0 h_i^2}{\sigma^2} + \eta\sum_{\ell=1}^{i-1}\left(\frac{g_{i,\ell}h_i}{h_\ell}\right)\gamma_\ell, \forall i \geq 1$ and $\gamma_0 = 0$, all independent of $\boldsymbol{\tau}$. As a result, the original optimization problem of $(\mathbf{P1})$ is equivalently recast as,

$$(\mathbf{P2}):\quad \max_{\boldsymbol{\tau}}\ \sum_{i=1}^{K}\omega_i\mathbf{e}_i^T\boldsymbol{\tau}\log_2\left(1+\gamma_i\frac{\mathbf{e}_0^T\boldsymbol{\tau}}{\mathbf{e}_i^T\boldsymbol{\tau}}\right), \tag{11}$$

$$\text{s.t.}\quad \boldsymbol{\tau}\in\mathcal{D}, \tag{12}$$

$$\omega_i \geq 0,\quad i=1,2,\ldots,K \tag{13}$$

where $\mathcal{D}$ denotes the feasible set of $\boldsymbol{\tau}$ specified by the constraints (6)–(7).

We note that the Hessian of $R_i(\boldsymbol{\tau}) = \mathbf{e}_i^T\boldsymbol{\tau}\log_2(1+\gamma_i\frac{\mathbf{e}_0^T\boldsymbol{\tau}}{\mathbf{e}_i^T\boldsymbol{\tau}})$ is negative semidefinite for any $\boldsymbol{\tau}$ as $\mathbf{x}^T\bigtriangledown^2 R_i(\boldsymbol{\tau})\mathbf{x} = \frac{-\gamma_i^2}{\mathbf{e}_i^T\boldsymbol{\tau}(\mathbf{e}_i^T\boldsymbol{\tau}+\gamma_i\mathbf{e}_0^T\boldsymbol{\tau})^2}(\mathbf{e}_0^T\mathbf{x}\cdot\mathbf{e}_i^T\boldsymbol{\tau} - \mathbf{e}_i^T\mathbf{x}\cdot\mathbf{e}_0^T\boldsymbol{\tau})^2 \leq 0$ for any real $(K+1)\times 1$ vector $\mathbf{x}$, which indicates that the objective function of $(\mathbf{P2})$ is concave with respect to $\boldsymbol{\tau}$. This is because a nonnegative weighted sum of concave functions is concave [15]. In addition to this, all constraints are linear inequalities, which indicates that the feasible set $\mathcal{D}$ is also concave. Thus, $(\mathbf{P2})$ is a convex optimization problem that can be efficiently solved by convex optimization tools. In Lemma 2, we provide a closed form solution to the problem $(\mathbf{P2})$, which in turn is similar to one presented in [6].

Lemma 2: An optimal time allocation $\boldsymbol{\tau}^\star$ of the problem $(\mathbf{P2})$ is given by

$$\mathbf{e}_i^T\boldsymbol{\tau}^\star = \begin{cases}\dfrac{1}{1+\sum_{\ell=1}^{K}(\gamma_\ell/z_\ell^\star)}, & i=0\\[2ex] \dfrac{\gamma_i/z_i^\star}{1+\sum_{\ell=1}^{K}(\gamma_\ell/z_\ell^\star)}, & i=1,\ldots,K\end{cases} \tag{14}$$

where $z_i^\star$ is the solution of the following two equations:

$$\ln(1+z_i) - \frac{z_i}{1+z_i} = \frac{\mu^\star}{\omega_i}\ln 2,\quad \forall i \tag{15}$$

$$\sum_{i=1}^{K}\frac{\omega_i\gamma_i}{1+z_i} = \mu^\star\ln 2. \tag{16}$$

The positive constant $\mu^\star$ is set to satisfy the above conditions for a given z_i.

Proof: Since $(\mathbf{P2})$ is a convex optimization problem, the corresponding Karush-Kuhn-Tucker (KKT) conditions are sufficient for global optimality. It can be easily shown that by solving the conditions the optimal $\boldsymbol{\tau}^\star$ is uniquely given as in (14), and this proof is essentially similar to the proof in [6, Appendix F]. Due to space limitations we omit the detailed derivation of (14). It must be noted that (14) is also an optimal solution to the original problem $(\mathbf{P1})$.

IV. A Total Transmission Time Minimization

In this section, we aim to minimize the total transmission time of the cooperative WPCN under minimum rate constraints. This problem can be formulated as

$$(\mathbf{P3}):\quad \min_{\boldsymbol{\tau}}\ \mathbf{1}^T\boldsymbol{\tau}, \tag{17}$$

$$\text{s.t.}\quad \mathbf{e}_i^T\boldsymbol{\tau} > 0,\quad i=0,1,\ldots,K, \tag{18}$$

$$R_i(\boldsymbol{\tau}) \geq \theta_i,\quad i=1,2,\ldots,K, \tag{19}$$

where $\theta_i(>0)$ is the minimum rate requirement of user i.

Recall that $R_i(\boldsymbol{\tau})$ is a concave function, and thus the feasible set specified by constraints in (19) forms a convex set. In addition, the objective and constraint functions are linear. Therefore, $(\mathbf{P3})$ is a convex optimization problem. The Lagrangian of $(\mathbf{P3})$ can be expressed as[7]

$$\mathcal{L}(\boldsymbol{\tau},\boldsymbol{\lambda}) = \mathbf{1}^T\boldsymbol{\tau} + \sum_{i=1}^{K}\lambda_i\left(\theta_i - \mathbf{e}_i^T\boldsymbol{\tau}\log_2\left(1+\gamma_i\frac{\mathbf{e}_0^T\boldsymbol{\tau}}{\mathbf{e}_i^T\boldsymbol{\tau}}\right)\right),$$

where λ_i is a non-negative Lagrangian dual variable associated with the ith constraint in (19).

It can be argued that the set of constraints (19) should be met with equality in the optimal solution, which follows from Lemma 3 below.

Lemma 3: An optimal time allocation $\boldsymbol{\tau}^\star$ of $(\mathbf{P3})$ must satisfy all the K constraints given in (19) with equality, i.e., $\mathbf{e}_i^T\boldsymbol{\tau}\log_2(1+\gamma_i\frac{\mathbf{e}_0^T\boldsymbol{\tau}}{\mathbf{e}_i^T\boldsymbol{\tau}}) = \theta_i, i=1,2,\ldots,K$.

Proof: We will prove this by contradiction. Suppose that $\boldsymbol{\tau}^\star = [\tau_0^\star,\ \tau_1^\star,\ldots,\tau_K^\star]^T$ is an optimal solution satisfying $\mathbf{e}_i^T\boldsymbol{\tau}^\star\log_2(1+\gamma_i\frac{\mathbf{e}_0^T\boldsymbol{\tau}^\star}{\mathbf{e}_i^T\boldsymbol{\tau}^\star}) > \theta_i$. Note that for $i\geq 1$, $\mathbf{e}_i^T\boldsymbol{\tau}\log_2(1+\gamma_i\frac{\mathbf{e}_0^T\boldsymbol{\tau}}{\mathbf{e}_i^T\boldsymbol{\tau}})$ is a monotonically increasing function of $\tau_i \geq 0$ for any given strictly positive γ_i and τ_0. This is because its derivative with respect to τ_i is nonnegative, i.e., $\frac{1}{\ln 2}[\ln(1+\gamma_i\frac{\mathbf{e}_0^T\boldsymbol{\tau}}{\mathbf{e}_i^T\boldsymbol{\tau}}) - \frac{\gamma_i\mathbf{e}_0^T\boldsymbol{\tau}}{\mathbf{e}_i^T\boldsymbol{\tau}+\gamma_i\mathbf{e}_0^T\boldsymbol{\tau}}] \geq 0$ due to $\frac{\partial h(x)}{\partial x} = \frac{x}{(1+x)^2} \geq 0$ and $\lim_{x\to 0^+} h(x) = 0$ for $x \triangleq \gamma_i\frac{\mathbf{e}_0^T\boldsymbol{\tau}}{\mathbf{e}_i^T\boldsymbol{\tau}} \geq 0$, where $h(x) = \ln(1+x) - \frac{x}{1+x}$. As a result, there exists $\tilde{\boldsymbol{\tau}} = [\tau_0^\star,\ \tilde{\tau}_1,\cdots,\tilde{\tau}_K]^T$ with $\tau_i^\star - \tilde{\tau}_i > 0$ for some $i\ (\geq 1)$ such that $\mathbf{e}_i^T\tilde{\boldsymbol{\tau}}\log_2(1+\gamma_i\frac{\mathbf{e}_0^T\tilde{\boldsymbol{\tau}}}{\mathbf{e}_i^T\tilde{\boldsymbol{\tau}}}) = \theta_i$. This is a contradiction to the assumption that $\boldsymbol{\tau}^\star$ is an optimal value for $(\mathbf{P3})$ owing to $\mathbf{1}^T\tilde{\boldsymbol{\tau}} \leq \mathbf{1}^T\boldsymbol{\tau}^\star$.

Taking into account the observation in Lemma 3, the following KKT conditions must be satisfied by optimal primal and dual solutions of $(\mathbf{P3})$:

$$\mathbf{e}_i^T\boldsymbol{\tau}^\star\log_2\left(1+\gamma_i\frac{\mathbf{e}_0^T\boldsymbol{\tau}^\star}{\mathbf{e}_i^T\boldsymbol{\tau}^\star}\right) = \theta_i,\quad \forall i\geq 1, \tag{20}$$

$$\frac{\partial\mathcal{L}(\boldsymbol{\tau}^\star,\boldsymbol{\lambda})}{\partial\mathbf{e}_i^T\boldsymbol{\tau}} = 0 \ \Rightarrow\ \lambda_i^\star\ln\left(1+\gamma_i\frac{\mathbf{e}_0^T\boldsymbol{\tau}^\star}{\mathbf{e}_i^T\boldsymbol{\tau}^\star}\right) - \frac{\lambda_i^\star\gamma_i\mathbf{e}_0^T\boldsymbol{\tau}^\star}{\mathbf{e}_i^T\boldsymbol{\tau}^\star+\gamma_i\mathbf{e}_0^T\boldsymbol{\tau}^\star} = \ln 2,\quad \forall i\geq 1, \tag{21}$$

$$\frac{\partial\mathcal{L}(\boldsymbol{\tau}^\star,\boldsymbol{\lambda})}{\partial\mathbf{e}_0^T\boldsymbol{\tau}} = 0 \ \Rightarrow\ \sum_{i=1}^{K}\frac{\lambda_i^\star\gamma_i\mathbf{e}_i^T\boldsymbol{\tau}^\star}{\mathbf{e}_i^T\boldsymbol{\tau}^\star+\gamma_i\mathbf{e}_0^T\boldsymbol{\tau}^\star} = \ln 2, \tag{22}$$

$$\lambda_i^\star > 0,\quad \forall i\geq 1. \tag{23}$$

By changing variables as $z_i = \gamma_i\frac{\mathbf{e}_0^T\boldsymbol{\tau}^\star}{\mathbf{e}_i^T\boldsymbol{\tau}^\star}, i=1,2,\ldots,K, \tilde{\lambda}_i^\star = \frac{\lambda_i}{\ln 2}$, and $\tilde{\theta}_i = \theta_i\ln 2$, the conditions (21)–(22) can be

$$\ln(1+z_i) - \frac{z_i}{1+z_i} = \frac{1}{\tilde{\lambda}_i^\star},\quad \forall i \tag{24}$$

$$\sum_{i=1}^{K}\frac{\tilde{\lambda}_i^\star\gamma_i}{1+z_i} = 1. \tag{25}$$

[7]To save effort, we ignore the set of non-negative constraints (18), then we will check whether the optimal solution always satisfies the constraints.

Algorithm 1: An efficient algorithm to solve $(\mathbf{P3})$.

```
initialize e_i^T τ ≥ 0, ∀i, endpoint values τ_ℓ, τ_u for e_0 τ
repeat
    e_0 τ ← (τ_l + τ_u)/2
    if f(z) − 1 > δ then
        τ_ℓ ← e_0 τ
    else
        τ_u ← e_0 τ
    end
    update e_i τ, ∀i > 0 from (27)
until |f(z) − 1| < δ, where δ > 0 is an error tolerance;
```

In addition, from (23), (24) and (25) it follows that

$$1 = \sum_{i=1}^{K} \frac{1}{\max\left(0, \ln(1+z_i) - \frac{z_i}{1+z_i}\right)} \frac{\gamma_i}{1+z_i}$$

$$\overset{(a)}{=} \sum_{i=1}^{K} \frac{\gamma_i}{(1+z_i)\ln(1+z_i) - z_i} \triangleq f(\mathbf{z}), \qquad (26)$$

where (a) follows from the same line of reasoning as that in the proof for Lemma 3, i.e., $h(x) \geq 0$. Also, the constraint specified in (20) can be rewritten as

$$\mathbf{e}_0^T \boldsymbol{\tau}^\star = \frac{1}{\gamma_i} \mathbf{e}_i^T \boldsymbol{\tau}^\star \left(e^{\frac{\tilde{\theta}_i}{\mathbf{e}_i^T \boldsymbol{\tau}^\star}} - 1 \right), \quad \forall i. \qquad (27)$$

Given $\tilde{\theta}_i$ and γ_i, an optimal solution $\boldsymbol{\tau}^\star$ can be computed from (26) and (27) by the following observation. Note that from Lemma 4 (provided in the final part of this section), $\mathbf{e}_0^T \boldsymbol{\tau}^\star$ and $\mathbf{e}_i^T \boldsymbol{\tau}^\star$ vary inversely, which implies that z_i varies directly as the single parameter $\mathbf{e}_0^T \boldsymbol{\tau}^\star$ only according to the definition of z_i. In addition, $f(\mathbf{z})$ is a monotonically decreasing function of $\mathbf{z}$ since the ith component of $\triangledown f(\mathbf{z})$ is $-\gamma_i \frac{\frac{z_i}{1+z_i} + h(z_i)}{h(z_i)^2 (1+z_i)^2} = -\frac{\gamma_i \ln(1+z_i)}{(h(z_i)(1+z_i))^2} < 0$, $\forall \mathbf{z} \succeq 0$, resulting in $\triangledown f(\mathbf{z}) \preceq 0$. Accordingly, z_i can be obtained by iteratively updating $\mathbf{e}_0^T \boldsymbol{\tau}$ and $\mathbf{e}_i^T \boldsymbol{\tau}$ from (27) until (26) is satisfied, which can be formulated as a single variable problem and solved by a line search strategy [15] effectively. To be more specific, when $f(\mathbf{z}) - 1$ is positive, $\mathbf{e}_0^T \boldsymbol{\tau}^\star$ is increased and otherwise it is decreased. To summarize, the algorithm to find the *optimal* solution to $(\mathbf{P3})$ is given in Algorithm 1.

An alternative closed form expression of the optimal solution to $(\mathbf{P3})$ can be obtained by rearranging (27) as follows:

$$\mathbf{e}_i^T \boldsymbol{\tau}^\star = \begin{cases} \dfrac{\tilde{\theta}_1 z_1^\star}{\ln(1+\gamma_1 z_1^\star)}, & i = 0 \\ \dfrac{\tilde{\theta}_i}{\ln(1+\gamma_i z_i^\star)}, & i = 1, \ldots, K \end{cases} \qquad (28)$$

where $z_i^\star$ (≥ 0) is tuned such that the condition (26) is met. It is worth noting that $\mathbf{e}_i^T \boldsymbol{\tau}^\star \geq 0$ always holds as long as $\theta_i \geq 0$.

Lemma 4: For given positive real numbers $c_i, \forall i$, $t(x) \triangleq c_1 x \left(e^{\frac{c_2}{x}} - 1\right)$ is a monotonically decreasing function of $x \geq 0$.

Proof: To prove this lemma, we need to show that the sign of the derivative of the function $t(x)$ with respect to x is negative. This can be seen that

$$\frac{\partial t(x)}{\partial x} = c_1\left(e^{\frac{c_2}{x}} - 1\right) - c_1 c_2 \frac{e^{\frac{c_2}{x}}}{x}$$

$$= c_1 e^{\frac{c_2}{x}} \left(1 - \frac{c_2}{x}\right) - c_1$$

$$\overset{(a)}{\leq} 0, \qquad (29)$$

where (a) comes from $e^{\frac{c_2}{x}}\left(1 - \frac{c_2}{x}\right) \leq 1$, which is equivalent to $1 - \bar{x} \leq e^{-\bar{x}}$ with $\bar{x} = \frac{c_2}{x} \geq 0$. It is worth noting that the last inequality can be proved by showing $\frac{\partial g(\bar{x})}{\partial \bar{x}} = -e^{-\bar{x}} + 1 \geq 0$ and $g(0) = 0$, where $g(\bar{x}) \triangleq e^{-\bar{x}} + \bar{x} - 1$.

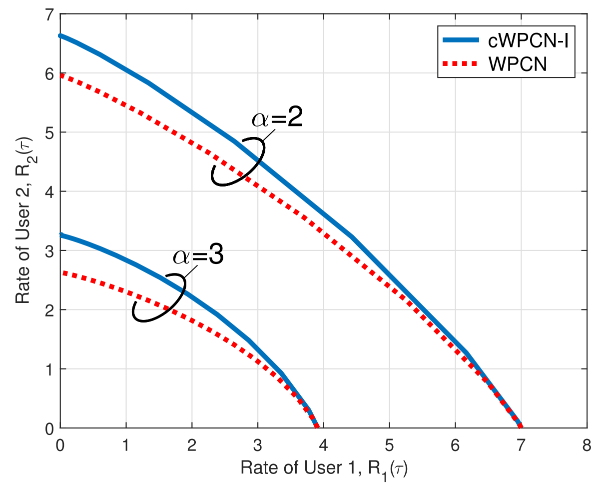

Fig. 2. Rate region comparison for WPCN and cooperative WPCN with $d_1 = 4, d_2 = 5$ according to different values of the pathloss exponent α.

V. Simulation Results

In this section, numerical results are provided to evaluate the performance gains of two proposed cooperative WPCN methods in comparison to non-cooperative WPCN schemes. We deploy a two-user channel setup (i.e., $K = 2$), where the distance between the H-AP and user i is d_i meters. For a fair comparison, it is assumed that each user has no access to the codebook used by other users. In the simulations, the transmit power at the H-AP is 30 dBm. The noise spectral density at the H-AP is assumed to be –160 dBm/Hz; the system bandwidth is set to 1 MHz. For ease of exposition, a simple path loss model [6] is considered, which is given as $h_i = \Gamma / d_i^\alpha$ and $g_{i,\ell} = \Gamma_g / d_i^\alpha$. Note that Γ refers to an average power attenuation at a reference distance of 1 m for the links between the H-AP and users including antenna gains, and Γ_g refers to the average power attenuation for the links among the users including antenna gains. Here, we set $\Gamma = -30$ dB and $\Gamma_g = -3$ dB to capture the effects of line-of-sight (LoS) and non-LoS for the different links.[8] Finally, the energy harvesting efficiency is set to be $\eta = 0.75$ for each user.

In Fig. 2, we compare the rate regions of the proposed cooperative WPCN in Section III (labeled ‘cWPCN-I’) and conventional WPCN with optimized time allocation [6] (labeled ‘WPCN’) for a given transmission time ($\sum_{i=0}^{K} \tau_i = 1$). It can be seen that the rate region is strictly

[8] It is assumed that the two users are sufficiently close to each other thanks to proper scheduling so that the propagation from one user to the other nearby user is highly likely to be under an LoS condition, contrary to the links between the H-AP and users.

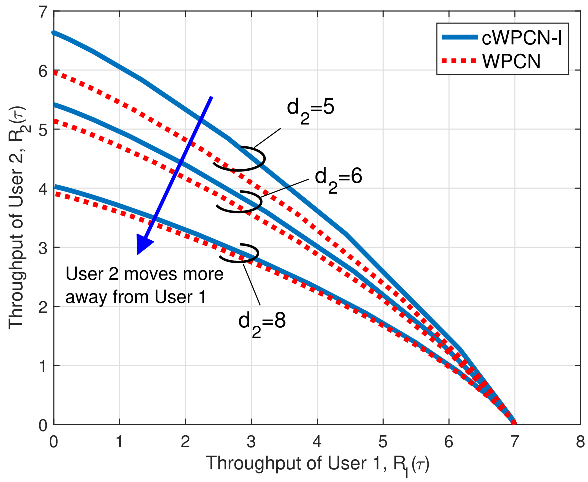

Fig. 3. Rate region comparison for different WPCN protocols and different distances between users with $d_1 = 4$ and $\alpha = 2$.

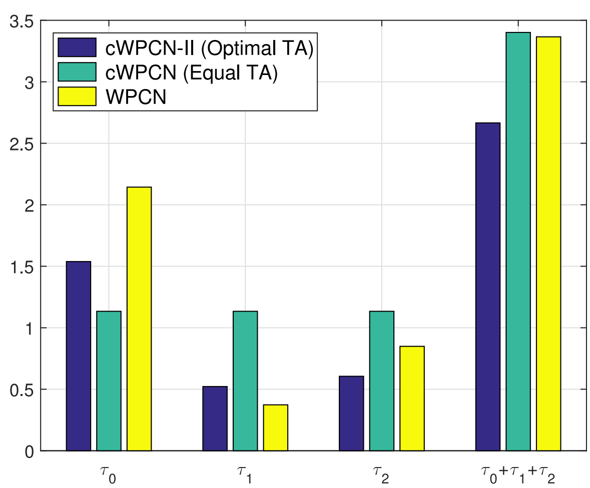

Fig. 4. Optimal time allocation comparison for different WPCN scenarios when $d_1 = 9$ and $d_2 = 10$.

enlarged by scavenging energy from interference. This is particularly due to the improvement of the far user's (user 2) rate, regardless of α. From the figure, it is evident that the proposed user cooperation also improves user fairness. In addition, it can be seen in Fig. 3 that the performance gain decreases with increasing d_2 for the fixed d_1. This is because when the users are relatively far away from each other, the amount of harvested energy from interference harvesting becomes negligibly small due to the higher path loss.

Fig. 4 plots the amount of transmission time at the H-AP (τ_0) and the two users (τ_1 and τ_2) as well as the total amount of time for different WPCN scenarios under minimum rate requirements, $\theta_1 = \theta_2 = 1$ (e.g., one-bit control message for IoT systems). We plot the transmission time of the cooperative WPCN proposed in Section IV (labeled 'cWPCN-II') and that of the conventional WPCN by setting $g_{i,\ell} = 0, \forall i, \ell$ in Algorithm 1. For the purpose of comparison, we also provide the performance of a suboptimal solution by assuming that equal amounts of time are allocated, i.e., $\tau_0 = \tau_1 = \tau_2$. It can be shown that the solution is given as $\tau = \max_i \frac{\theta_i}{\log_2(1+\gamma_i)}$. This suboptimal time allocation approach is labeled as 'cWPNC (Equal TA)'. For the extra equality constraint, an amount of time for some users is most likely not to be fully necessary to maintain their minimum rate requirements; and thus, the total amount of time is even longer than that of the proposed cWPCN-II method and conventional WPCN with optimized time allocation. It is observed that cWPCN-II requires a fairly less amount of total transmission time, compared to other two suboptimal solutions.

Remark 1: We should highlight that cWPCN-I and cWPCN-II work properly regardless of user orderings. Finding the optimal scheduling is NP-hard in general since it has to consider not only the direct channel gains between the H-AP and users but also the channel gains among user. However, in the special case of two users used in the simulation, our sorting approach based on the direct channel gains is optimal. It would be interesting to investigate efficient scheduling algorithms for a general case, and we leave this for future work.

VI. Conclusion

We proposed a novel cooperative WPCN protocol which exploits interference as a new source of energy harvesting at the users. We characterized the maximum weighted sum-rate and the minimum total transmission time in closed forms by jointly optimizing time allocations for the downlink and the uplink channels. Through the numerical results, it has been shown that the proposed protocol has a great potential to overcome the doubly near-far problem, which is arguably the most challenging issue in WPCN.

References

[1] X. Lu, P. Wang, D. Niyato, D. I. Kim, and Z. Han, "Wireless networks with RF energy harvesting: A contemporary survey," *IEEE Commun. Surveys Tut.*, vol. 17, no. 2, pp. 757–789, Apr.–Jun. 2015.

[2] S. Ulukus *et al.*, "Energy harvesting wireless communications: A review of recent advances," *IEEE J. Sel. Areas Commun.*, vol. 33, no. 3, pp. 360–381, Mar. 2015.

[3] T. A. Khan, A. Alkhateeb, and R. W. Heath, "Millimeter wave energy harvesting," *IEEE Trans. Wireless Commun.*, vol. 15, no. 9, pp. 6048–6062, Sep. 2016.

[4] K. Huang and V. K. N. Lau, "Enabling wireless power transfer in cellular networks: Architecture, modeling and deployment," *IEEE Trans. Wireless Commun.*, vol. 13, no. 2, pp. 902–912, Feb. 2014.

[5] S. Bi, Y. Zeng, and R. Zhang, "Wireless powered communication networks: An overview," *IEEE Wireless Commun.*, vol. 23, no. 2, pp. 10–18, Apr. 2016.

[6] H. Ju and R. Zhang, "Throughput maximization in wireless powered communication networks," *IEEE Trans. Commun.*, vol. 13, no. 1, pp. 418–428, Jan. 2014.

[7] L. Liu, R. Zhang, and K.-C. Chua, "Multi-antenna wireless powered communication with energy beamforming," *IEEE Trans. Commun.*, vol. 62, no. 12, pp. 4349–4361, Dec. 2014.

[8] P. D. Diamantoulakis, K. N. Pappi, Z. Ding, and G. K. Karagiannidis, "Wireless-powered communications with non-orthogonal multiple access," *IEEE Trans. Wireless Commun.*, vol. 15, no. 12, pp. 8422–8436, Dec. 2016.

[9] P. D. Diamantoulakis, K. N. Pappi, G. K. Karagiannidis, H. Xing, and A. Nallanathan, "Joint downlink/uplink design for wireless powered networks with interference," *IEEE Access*, vol. 5, pp. 1534–1547, 2017.

[10] H. Ju and R. Zhang, "User cooperation in wireless powered communication networks," in *Proc. IEEE Global Commun. Conf.*, Dec. 2014, pp. 1430–1435.

[11] H. Chen, Y. Li, J. L. Rebelatto, B. F. Uchôa-Filho, and B. Vucetic, "Harvest-then-cooperate: Wireless-powered cooperative communications," *IEEE Trans. Signal Process.*, vol. 63, no. 7, pp. 1700–1711, Apr. 2015.

[12] A. Biason and M. Zorzi, "Transmission policies in wireless powered communication networks with energy cooperation," in *Proc. Eur. Signal Process. Conf.*, Budapest, Hungary, Aug. 2016, pp. 592–596.

[13] K. Ishibashi, H. Ochiai, and V. Tarokh, "Energy harvesting cooperative communications," in *Proc. IEEE Int. Symp. Pers. Indoor Mobile Radio Commun.*, Sydney, NSW, Australia, Sept. 2012, pp. 1819–1823.

[14] S. Sudevalayam and P. Kulkarni, "Energy harvesting sensor nodes: Survey and implications," *IEEE Commun. Surveys Tut.*, vol. 13, no. 3, pp. 443–461, Jul.–Sep. 2011.

[15] S. Boyd and L. Vandenberghe, *Convex Optimization*. Cambridge, U.K.: Cambridge Univ. Press, 2004.